Applied Energy 200 (2017) 141–154

Contents lists available at ScienceDirect

Applied Energy

journal homepage: www.elsevier.com/locate/apenergy

Parameter estimation of photovoltaic cells using an improved chaotic whale optimization algorithm

Diego Oliva [a,b,e,*], Mohamed Abd El Aziz [c,e,f], Aboul Ella Hassanien [d,e]

[a] Departamento de Ciencias Computacionales, Tecnológico de Monterrey, Campus Guadalajara, Av. Gral. Ramón Corona 2514, Zapopan, Jal, Mexico
[b] Departamento de Ciencias Computacionales, Universidad de Guadalajara, CUCEI, Av. Revolución 1500, Guadalajara, Jal, Mexico
[c] Department of Mathematics, Faculty of Science, Zagazig University, Zagazig, Egypt
[d] Faculty of Computers Information, Cairo University, Cairo, Egypt
[e] Scientific Research Group in Egypt (SRGE), Egypt[1]
[f] School of Computer Science and Technology, Wuhan University of Technology, Wuhan, China

HIGHLIGHTS

- We modify the whale algorithm using chaotic maps.
- We apply a chaotic algorithm to estimate parameter of photovoltaic cells.
- We perform a study of chaos in whale algorithm.
- Several comparisons and metrics support the experimental results.
- We test the method with data from real solar cells.

ARTICLE INFO

Article history:
Received 22 January 2017
Received in revised form 30 April 2017
Accepted 3 May 2017
Available online 12 May 2017

Keywords:
Photovoltaic cells
Whale optimization
Chaotic maps
Solar cell modeling
Parameter estimation

ABSTRACT

The using of solar energy has been increased since it is a clean source of energy. In this way, the design of photovoltaic cells has attracted the attention of researchers over the world. There are two main problems in this field: having a useful model to characterize the solar cells and the absence of data about photovoltaic cells. This situation even affects the performance of the photovoltaic modules (panels). The characteristics of the current vs. voltage are used to describe the behavior of solar cells. Considering such values, the design problem involves the solution of the complex non-linear and multi-modal objective functions. Different algorithms have been proposed to identify the parameters of the photovoltaic cells and panels. Most of them commonly fail in finding the optimal solutions. This paper proposes the Chaotic Whale Optimization Algorithm (CWOA) for the parameters estimation of solar cells. The main advantage of the proposed approach is using the chaotic maps to compute and automatically adapt the internal parameters of the optimization algorithm. This situation is beneficial in complex problems, because along the iterative process, the proposed algorithm improves their capabilities to search for the best solution. The modified method is able to optimize complex and multimodal objective functions. For example, the function for the estimation of parameters of solar cells. To illustrate the capabilities of the proposed algorithm in the solar cell design, it is compared with other optimization methods over different datasets. Moreover, the experimental results support the improved performance of the proposed approach regarding accuracy and robustness.

1. Introduction

The air pollution is a situation that affects all the countries in the world. Along decades, fossil fuels have been used as energy sources. However, their using has affected the cities of several countries. Nowadays, the effects of the abuse on using this kind of energy sources are reflected in the global warmness. As a result, many nations put more attention to renewable energies. One of the

* Corresponding author at: Departamento de Ciencias Computacionales, Tecnológico de Monterrey, Campus Guadalajara, Av. Gral. Ramón Corona 2514, Zapopan, Jal, Mexico.
E-mail addresses: diego.oliva@itesm.mx, diego.oliva@cucei.udg.mx (D. Oliva), abd_el_aziz_m@yahoo.com (M. Abd El Aziz), aboitcairo@gmail.com (A. Ella Hassanien).
[1] www.egyptscience.net.

http://dx.doi.org/10.1016/j.apenergy.2017.05.029
0306-2619/

most efficient renewable sources is the solar energy that is currently explored, and it is used to contribute in the rising demands for energy supplies. According to [1], the solar photovoltaic (PV) power generation technology had a new record in the world in 2015, increasing their capacities 25% up to 2014. Moreover, PV is an emission-free distributed generation system that is able to directly convert solar energy to electricity and supply power for specific purposes. Solar energy has several advantages compared with other typical sources. However, it has some disadvantages that represent open research problems. The main drawbacks of PV energy are the high initial investment and the low efficiency of the solar cells [2]. In the same way, since PV modules are outdoors, the energy is affected by weather. This fact also implies to a high cost of the maintenance and the replacement of modules [3,4].

The efficacy of the solar cells (SC) system is affected by weather and its design [3,4]. Considering such situations, an accurate design of PV cells is a crucial and challenging task in this field. There are two basic steps for modeling the PV cells: (1) the mathematical model formulation and (2) The estimation accuracy of PV cells parameter values. On the mathematical model, there are characteristics of the Current vs. Voltage (*I-V*) that dominates the SC behavior. Several mathematical approaches have been developed to describe the nonlinearity performance of the PV systems [5–12]. In practical terms, the single diode (SD) model and double diode (DD) model are equivalent electronic circuits that are extremely used to define a solar cell. The SD model that has five unknown parameters and the DD model which is required to find seven unknown parameters [13,14]. Regardless of the selected model, it is necessary to estimate or identify the photo-generated current, the diode saturation current, the series resistance, and the diode ideality factor. Such parameters directly affect the performance of the SC and photovoltaic panels. The biggest problem could be established as determining the optimal values of parameters which are applied to the selected model and approximate the results of the experimental data from the real SC [13].

The problem of identifying the PV cells parameters should be defined from an optimization point of view. In other words, it is necessary to specify an objective function based on the characteristics of the *I-V* of the SC. Considering the data is commonly obtained from the measurements, it has a certain degree of noise. The resultant search space produced by the objective function is high multimodal and complex to be solved by the classical algorithms that involve gradient operators [15–17].

The deterministic approaches are the most conventional or classic methodologies to estimate the PV parameters. For example, the least squares (Newton-based approach) [18], Lambert W-functions [19,20], the iterative curve fitting [21] and tabular method [22]. There exist some interesting studies that analyze different methods [23,24]. The using of the deterministic techniques implies to several model restrictions such as differentiability and convexity to be correctly applied [23]. Therefore, their outputs are affected by the initial solutions, which lead to local optima. For example, the application of the Newton-Rapson method [25] to the DD model, which presents a large deviation among the real, and the estimated of the current and voltage values [26]. The stochastic methods are an alternative efficient solution that avoids the situation presented by deterministic algorithms. In this group, they included the heuristic and the metaheuristic approaches that can solve complex problems considering simple initial conditions. In specifically, the results of metaheuristic algorithms are better than those which are based on deterministic methods considering robustness and accuracy [13,27–33]. In the related literature, they are exist several implementations to solve the solar cells parameter identification problem. Such methods include Genetic Algorithms (GA) [28,34], Particle Swarm Optimization (PSO) [10,35], Simulated Annealing (SA) [29], Harmony Search (HS) [13], Bacterial Foraging Algorithm (BFA) [30], Simplified Teaching-Learning Based Optimization (STBLO) [36] and Cat Swarm Optimization (CSO) [37]. Although heuristic methods present a higher probability of obtaining a global solution in comparison with deterministic ones, they have critical limits [27]. For example, the No Free Lunch (NFL) theorem that has been logically proved, states that not all the optimization algorithms can be used to solve all the problems [38]. Meanwhile, a considerable amount of metaheuristic methods have several parameters that should be experimentally tuned. This fact affects their efficacy and accuracy. On the other hand, depending on the search surface, the algorithms could be trapped into local optimal values, and their performance is degraded along the iterations. On the other hand, the design and the operators of each algorithm make it able to optimize some problems better. For example, in the case of the classical PSO and GA, they maintain a trend that concentrates toward local optima, since their elitist mechanism forces premature convergence [39,40]. Such a behavior becomes worse when the optimization algorithm faces multi-modal functions [41,42]. Since the SA and HS use only one search agent, they are very sensitive to the initialization. The use of only one search element affects the probability of localizing the global optimal in multimodal search spaces in comparison with GA or PSO [43,44]. Therefore, HS, GA, SA, and PSO present a deficient performance in the application over noisy and multi-modal objective functions. Considering these circumstances most of the stochastic approaches presents a bad performance for this problem [45]. In the problem of parameter estimation of SC, the use of accurate optimization approaches affects the SC system design that is reflected on the cost reduction [14,22]. However, metaheuristic approaches are a good alternative since they can achieve optimal solutions using processes that are not computationally expensive.

In the context of the metaheuristic methods, the Whale Optimization Algorithm (WOA) [46] was recently proposed as an alternative one for the global optimization problems. The WOA is inspired by the hunting behavior of the humpback whales. The WOA generates a random group of initial solutions, in the optimization process, each candidate solution takes a new position in the search space considering as a reference, the best element of the group. Some internal parameters are used to generate the whale's behavior. According to the authors, the values of such parameters is adaptive in the iterative process, and they guarantee a good relationship between the exploration and the exploitation. The main advantage of WOA is the simulation of the mechanism to chase the prey using the randomness of the best search agents and the using of spiral to mimics the bubble-net attraction process of humpback whales [46]. This mechanism differs the WOA from the other similar approaches. On the other hand, the WOA possesses few parameters to set and also the most important parameters are self-tuning along the iterative process. Considering these facts, WOA has two main drawbacks, (1) its adaptive parameter depending on the random distribution and (2) like another metaheuristic (evolutionary and swarm) algorithms, it has a premature convergence. It happens especially in problems that possess high multimodal search spaces. The WOA has been tested over different benchmark functions and engineering design benchmark problems [46].

Recently, the chaos theory has more attention improving the performance of metaheuristic algorithms [47]. It is described as erratic behavior in nonlinear systems through using the chaotic maps. These maps are treated as particles which travel in a limited range of nonlinear and dynamic system without definite regularity traveling path of these particles. The chaotic sequence with high randomness improves the diversity of solutions and its convergence, these features have been tested after several studies in the related literature [47].

The aim of this paper is to present an attractive improved approach (and it is not for devising an SC algorithm that could beat all currently available methods) that is able to accurately estimate the best parameter of PV cells using circuit models. Based on the NFL theorem, a chaotic Whale Optimization Algorithm (CWOA) is proposed which it combines the features of the standard WOA with chaotic maps to improve its performance. The CWOA is used to find the set of parameters that models a SC. The using of chaos to generate the values used to compute the internal parameters of the WOA which leads to the optimization process avoids the local optimal values and improves their convergence speed. Moreover, this proposed method has less parameters to configure to find the best solution in the optimization process. In other word, less human interaction is necessary to obtain the optimal configuration of SC. In this sense, the novelty of the paper is the implementation of the CWOA and its using to estimate the parameters of solar cells using circuit models. Considering the above, the use of an accurate approach for the estimate the parameter of SC that possess mechanisms for self-tuning, increases the quality of the PV system design reducing the cost and maintain the amount of energy [14,22].

In order to test the proposed algorithm, it is applied for determining the parameters of solar cells. The proposed implementation considers the PV parameters as a candidate solution. Similar to other algorithms there are exist a set of candidate solutions. The quality of them is evaluated in terms of the objective function (Root Mean Square Error) that verifies whether if the estimated values are closer to the experimental data. Based on the objective function values, the position of each element of the set is modified considering the hunting and the bubble-net attracting mechanisms of humpback whales. The chaos here is used to control the internal variables of these processes. Following this methodology, they can find that the estimated parameters can produce the best approximation to the I–V measurements obtained by the true SC. All the performed experiments use three datasets extracted from real photovoltaic modules [48], in this way the CWOA is applied for a real life problem. In order to illustrate the efficiency of the proposed approach, it is compared with other similar optimization methods. Such methods are: Newton-based method [18], HS [13], Grouping-Based Global Harmony Search (GGHS) [13], Innovative Global Harmony Search (IGHS) [13], DE [32], Levenberg–Marquardt algorithm combined with simulated annealing (LMSA) [49], Artificial Bee Swarm Optimization (ABSO) [50], Pattern Search (PS) [51], SA [29], Bird Matting Optimizer (BMO) [52], Chaos Particle Swarm Algorithm (CPSO) [35], Repaired Crossover Rate Adaptive DE (Rcr-IJADE) [32], STLBO [36], Generalized Oppositional Teaching Learning Based Optimization (GOTLBO) [53], Artificial Bee Colony (ABC) [54], CSO [37], and BFA [30]. Experimental evidence shows that CWOA is practically immune to the sensitivity generated by noisy conditions, and it has a high performance regarding accuracy and robustness.

The rest of this paper is organized as follows. In Section 2, the problem of solar cell identification is defined. Section 3 describes the WOA algorithm. Section 4 explains the chaotic systems. In Section 5, the proposed algorithm is introduced. Section 6 presents the experimental results and comparisons. Finally, in Section 7, the conclusions are presented.

2. Photovoltaic models

In order to generate a precise design of solar cells, it is necessary to have a good mathematical model. After that, it can be used a search strategy to estimate the best values for the model. In the literature, there are two typical models: one considers a Single Diode (SD) and another one that employs Double Diode (DD) [13]. This section describes the two models and how they can be adapted as objective functions.

2.1. Double diode model

The double diode (DD) model is firstly defined in the equivalent circuit presented in Fig. 1. This approach uses two diodes to shunt the photo-generated (I_{ph}) current source. One of these diodes is set as a rectifier and the second diode is used to model the charge recombination current and some non-idealities. The DD model also requires a resistor connected in series with the diodes [13,55].

In the circuit of Fig. 1, the current of the cell is computed using Eq. (1).

$$I_t = I_{ph} - I_{d1} - I_{d2} - I_{sh}, \tag{1}$$

where I_t is the terminal current, I_{ph} is the photo-generated current, I_{d1}, I_{d2} are the first and second diode currents, respectively, whereas I_{sh} is the shunt resistor current. For the proper modeling of PV cells, it used the Shockley diode equation. Hence, Eq. (1) is rewritten as shown in Eq. (2).

$$I_t = I_{ph} - I_{sd1}\left[\exp\left(\frac{q(V_t + R_s \cdot I_t)}{n_1 \cdot k \cdot T}\right) - 1\right] - I_{sd2}\left[\exp\left(\frac{q(V_t + R_s \cdot I_t)}{n_2 \cdot k \cdot T}\right) - 1\right] - \frac{V_t + R_s \cdot I_t}{R_{sh}}, \tag{2}$$

where I_{sd1} and I_{sd2} are the diffusion and saturation current, respectively. V_t is the terminal voltage whereas the series and shunt resistances are represented by R_s and R_{sh} respectively. In the Shockley diode equation, $q = 1.602 \times 10^{-19}$ (coulombs) is the magnitude of charge on an electron, $k = 1.380 \times 10^{-23}$ (J/K) is the Boltzmann constant, n_1 and n_2 are the diffusion and recombination diode ideality factors, respectively. Finally, T is the cell temperature (K). Therefore, Eq. (2) has seven unknown parameters (R_s, R_{sh}, I_{ph}, I_{sd1}, I_{sd2}, n_1, and n_2). The estimation or identification of such values provides a better performance of SC, for that reason, this task is crucial in PV systems.

2.2. Single diode model

From the DD model, I_{sd1} and I_{sd2} are the diffusion and saturation currents, respectively. The SD model uses a non-physical ideality factor n to represent I_{sd1} and I_{sd2} [13,27,29]. The equivalent circuit of single diode model is presented in Fig. 2, and it is commonly used in the related literature for PV modeling. It is a simple approach that has only five parameters to be estimated.

In the SD model, Eq. (2) is adapted as the following

$$I_t = I_{ph} - I_{sd}\left[\exp\left(\frac{q(V_t + R_s \cdot I_t)}{n \cdot k \cdot T}\right) - 1\right] - \frac{V_t + R_s \cdot I_t}{R_{sh}} \tag{3}$$

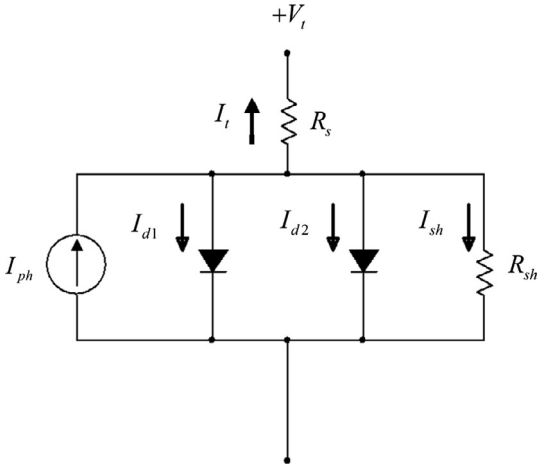

Fig. 1. Double diode model of solar cells [54,55].

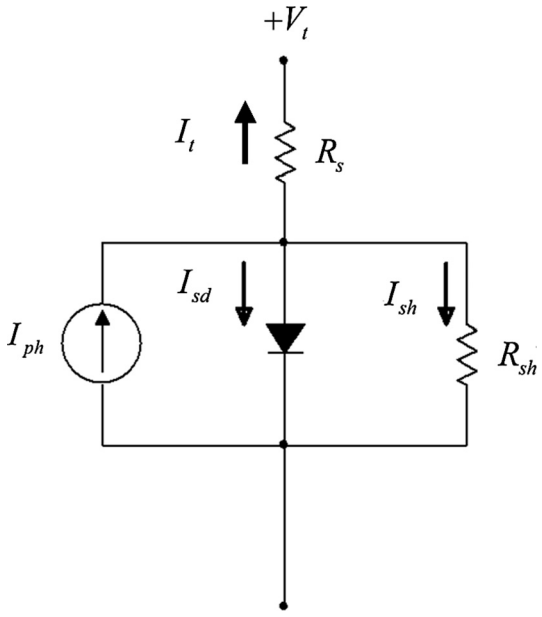

Fig. 2. Single diode model of solar cells [54,55].

Table 1
The range of the solar cell parameters.

Parameter	Lower value	Upper value
R_s (Ω)	0	0.5
R_{sh} (Ω)	0	100
I_{ph} (A)	0	1
I_{sd} (μA)	0	1
n	1	2

The parameters to be identified are R_s, R_{sh}, I_{ph}, I_{sd}, and n. Table 1 shows the ranges of SD and DD parameters. Notice that the values of I_{sd1} and I_{sd2} in the DD are the same as I_{sd} in the SD model. It is important to mention that the values of Table 1 are commonly used on the related literature [17,18,21,56,57].

2.3. Considering the solar cells design as an optimization problem

Using Eqs. (2) and (3), it is possible to estimate the parameters that modelphotovoltaic cells. However, in the presented approach, it is necessary to define an objective function to determine the quality of the estimated parameters. In other words, a good set of parameters produces an accurate approximation between the *I-V* measurements from the physical SC and the values from the mathematical model. The SD and the DD must be adapted in order to be used to measure the difference with regard to the experimental data. The error function of DD is then defined as [55]:

$$f_{\mathrm{DD}}(V_t, I_t, \mathbf{x}) = I_t - x_3 + x_4\left[\exp\left(\frac{q(V_t + x_1 \cdot I_t)}{x_6 \cdot k \cdot T}\right) - 1\right] + x_5\left[\exp\left(\frac{q(V_t + x_1 \cdot I_t)}{x_7 \cdot k \cdot T}\right) - 1\right] + \frac{V_t + x_1 \cdot I_t}{x_2}, \quad (4)$$

whereas for the SD model:

$$f_{\mathrm{SD}}(V_t, I_t, \mathbf{x}) = I_t - x_3 + x_4\left[\exp\left(\frac{q(V_t + x_1 \cdot I_t)}{x_5 \cdot k \cdot T}\right) - 1\right] + \frac{V_t + x_1 \cdot I_t}{x_2} \quad (5)$$

From Eqs. (4) and (5), the values of V_t and I_t are experimentally collected from the solar cell. Meanwhile, $\mathbf{x}$ is a vector with the parameter of the model and is defined as: $\mathbf{x} = [R_s, R_{sh}, I_{ph}, I_{sd1}, I_{sd2}, n_1, n_2]$ for the double diode circuit and $\mathbf{x} = [R_s, R_{sh}, I_{ph}, I_{sd}, n]$ for the single diode circuit. The aim of f_{DD} and f_{SD} is to evaluate the grade of correspondence of the current values computed using $\mathbf{x}$ and a model with the real values defined by I_t. Then the optimization process concerns with minimizing such difference adjusting (or modifying) $\mathbf{x}$ at each iteration. In this context using a dataset of N_E elements, the objective function is the Root Mean Square Error (*RMSE*) which defined in Eq. (6).

$$RMSE(\mathbf{x}) = \sqrt{\frac{1}{N}\sum_{c=1}^{N_E}\left(f_M^c(V_t^c, I_t^c, \mathbf{x})\right)^2}, \quad (6)$$

From Eq. (6), M is used to select the model DD or SD. It is important to mention that the dataset could also be extracted from a commercial PV cell provided by the manufactured in a datasheet. Regardless how the data is obtained, it contains noise that affects directly the space where the objective function is defined. It contains a high multi-modal and noisy characteristics [15,16]. This fact affects the most of the proposed search strategies [45].

3. Whale optimization algorithm

The whale optimization algorithm (WOA) simulates the behavior of the humpback whales [46]. These whales search for the prey's location and attack them using one of two mechanisms: encircling them or creating bubble-nets. On the WOA optimization process when whales are looking for the prey, it is considered an exploration of the search space. Meanwhile, the attack behaviors represent the exploitation of the regions where there are exist more probabilities to find a solution.

In the original WOA, the bubble-net behavior is simulated as a spiral movement. The position of a whale is updated in a spiral by simulating the helix-shaped movement of the humpback whales around the prey as:

$$\mathbf{x}_w(t+1) = D \cdot e^{bl} \cdot \cos(2\pi l) + \mathbf{x}_p \quad (7)$$

where $D = |\mathbf{x}_p(t) - \mathbf{x}_w(t)|$ is the distance between a whale $\mathbf{x}_w(t)$ and prey $\mathbf{x}_p(t)$, t is the current iteration, b is a constant for defining the shape of the logarithmic spiral, l is a random number in $[-1, 1]$, and $(\cdot)$ is a multiplication of elements.

On the other hand, in the encircling behavior [46], the whales update their positions based on the best location as follows:

$$\begin{aligned} D &= |C \cdot \mathbf{x}_p(t) - \mathbf{x}_w(t)| \\ \mathbf{x}_w(t+1) &= \mathbf{x}_p(t) - A \cdot D \end{aligned} \quad (8)$$

where D represents the distance between whale and prey. The C and A are coefficient vectors and are computed using Eq. (9).

$$\begin{aligned} C &= 2r \\ A &= 2a \odot r - a \end{aligned} \quad (9)$$

where r is a random vector, and a is linearly decreased from 2 to 0 as the iterations proceed. The whales can swim around their prey simultaneously through a shrinking circle and along a spiral-shaped path. This process is modeled in Eq. (10).

$$\mathbf{x}_w(t+1) = \begin{cases} \mathbf{x}_p(t) - A \cdot D & \text{if } prob < 0.5 \\ D \cdot e^{bl} \cdot \cos(2\pi l) + \mathbf{x}_p(t) & \text{if } prob \geqslant 0.5 \end{cases} \quad (10)$$

where $prob \in t[1]$ represents the probability of choosing either the spiral model or shrinking encircling mechanism to update the position of whales. As well as the humpback whales in seas search randomly for prey. The location of a whale is modified by choosing a random whale instead of the best whale as follows:

$$\begin{aligned} D &= |C \cdot \mathbf{x}_{rand}(t) - \mathbf{x}_w(t)| \\ \mathbf{x}_w(t+1) &= \mathbf{x}_{rand}(t) - A \cdot D \end{aligned} \quad (11)$$

where $\mathbf{x}_{rand}(t)$ is a random position vector chosen from the current population. The $\mathbf{x}_p$ is updated by selecting the best solution from the population based on the objective function.

4. Chaotic system

In non-linear dynamic systems, the chaos is a deterministic and random-like process that is sensitive to the initial conditions. When the initial values present a small difference, the non-linear system has a large change in its behavior. In general terms, chaos has a fine internal structure, and chaotic systems have the following dynamic characteristics: Sensitivity to primary condition, Deterministic and Randomness. Based on these properties of chaotic systems, the population diversity can be maintained which avoids getting stuck in a local optimum and improves the quality of searching for global optimum [47,58].

The chaos can be defined as a discrete-time dynamical system presented in Eq. (12).

$$cp^i_{k+1} = f(cp^i_k), \qquad i = 1, 2, 3, \ldots . n \tag{12}$$

where n is the dimension of the map. $f(cp^i_k)$ is the function that generates the chaotic model and it is described using one of the maps presented in Table 2. Such maps are widely used in the related literature [58].

5. Chaotic Whale Optimization Algorithm (CWOA) for parameter estimation of solar cells

This section introduces the modification of the standard WOA using the Singer chaotic map. This hybrid approach is called Chaotic Whale Optimization Algorithm (CWOA). In comparison with WOA, the proposed method is able to avoid being trapped at the local optima and also its convergence speed is improved. In the CWOA, the value of parameter *prob* from Eq. (10) is modeled using the Singer map. This modification permits to control the selection of the spiral model or to shrink encircling mechanism to update the position of whales.

First, it is necessary to define the optimization problem. The parameters of each equivalent circuit (DD and SD) should be adapted as vectors that are considered as positions of whales. The number of parameters of the diode models defines the dimensionality of the optimization space. In order to address the SC parameter estimation as an optimization problem, the values of some of the variables should be limited. Such limits define the search space where an optimization algorithm (for example CWOA) is applied. For comparative and experimental purposes, the bounds used in this paper are widely used in similar works reported in the state-of-the-art [17,18,21,56,57]. In this sense, the bounds that generate the search space is presented in Eq. (13).

$$\begin{aligned}
&\text{minimize}: \ RMSE(\mathbf{X}), \ \mathbf{X} = [\mathbf{x}_{w1}, \mathbf{x}_{w2}, \ldots, \mathbf{x}_{wN}], \ \mathbf{x}_{wi} = [x_{i,1}, x_{i,2}, \ldots x_{i,d}] \ \ d \in [5,7], \\
&\text{subject to}: \\
&\qquad d = 5(\text{SD}) \qquad\qquad d = 7(\text{DD}) \\
&\qquad 0 \leqslant x_{i,1}(R_s) \leqslant 0.5 \qquad 0 \leqslant x_{i,1}(R_s) \leqslant 0.5 \\
&\qquad 0 \leqslant x_{i,2}(R_{sh}) \leqslant 100 \qquad 0 \leqslant x_{i,2}(R_{sh}) \leqslant 100 \\
&\qquad 0 \leqslant x_{i,3}(I_{ph}) \leqslant 1 \qquad 0 \leqslant x_{i,3}(I_{ph}) \leqslant 1 \\
&\qquad 0 \leqslant x_{i,4}(I_{sd}) \leqslant 1 \qquad 0 \leqslant x_{i,4}(I_{sd1}) \leqslant 1 \\
&\qquad 1 \leqslant x_{i,5}(n) \leqslant 2 \qquad 0 \leqslant x_{i,5}(I_{sd2}) \leqslant 1 \\
&\qquad\qquad\qquad\quad 1 \leqslant x_{i,6}(n_1) \leqslant 2 \\
&\qquad\qquad\qquad\quad 1 \leqslant x_{i,7}(n_2) \leqslant 2
\end{aligned} \tag{13}$$

The CWOA algorithm starts with generating a random population $\mathbf{X}$ of size N whales $\mathbf{x}_{wi}$ and dimension equal to the number of parameters of a selected model (d). Also the algorithm generates chaotic sequence *cp* from Singer map. At each iteration, a whale updates its position based on the fitness function called RMSE previously defined in Eq. (6). In the CWOA, the selection between the procedures of spiral model or shrinking encircling model to update the position of whales is done using a probability (*prob*) parameter. Unlike to WOA, the *prob* is taken from the chaotic sequence *cp*, in this way $prob(t) = cp(t)$. Any chaotic map from Table 2 can be considered to compute the sequence. According to Eq. (10), if $prob(t) < 0.5$, the position of a whale is updated using the encircling model otherwise, the position is calculated with the spiral model. The best position is selected according to the objective function, and it is also updated at each iteration. The entire process of CWOA is described in Algorithm 1 and Fig. 3.

From Algorithm 1, V_{tm} and I_{tm} are the voltage and current values measured (or obtained) form a real life photovoltaic cell, respectively. As stated previously in Section 2, in the objective function, such values are V_t and I_t and they could be extracted experimentally or provided by the manufacturer.

Table 2
Commonly used chaotic maps.

Map	Function
Sinusoidal	$p_{k+1} = ap_k^2 \sin(\pi p_k)$ $p_0 \in [0,1]$, $0 < a \leqslant 4$, k = Iteration number
Logistic	$p_{k+1} = ap(1-p_k)$ $p_k \in (0,1)$, considering that $p_0 \in [0,1]$, $\quad 0 < a \leqslant 4$ k = Iteration number
Singer	$p_{k+1} = \mu(7.86p_k - 23.31p_k^2 + 28.75p_k^3 - 13.3p_k^4)$ $p_k \in (0,1)$, considering that $p_0 \in (0,1)$, $\quad \mu \in [0.9, 1.08]$
Tent	$p_{k+1} = G(p_k)$ $G(p) = \begin{cases} \frac{p}{0.7}, & p < 0.7 \\ \frac{1}{0.3}p(1-p) & \text{otherwise} \end{cases}$

Algorithm 1: Chaotic Whale Optimization Algorithm (CWOA)

```
Input: d = dimension of each whale, V_tm, I_tm
Output: x_p (parameter estimation)
Initialize: itern = max number of iteration, f_p = best function,
  N = number of whales,
Generate a population of N whales x_wi, i = 1, 2, 3, ..., N
Compute the objective function RMSE = f_i of each whale x_wi
  using Eq. (6) and V_tm, I_tm
t = i
Generate Singer map cp with size equal to the number of
  iteration (itern)
do
  Decrease the value of a from 2 to 0
    for each whale x_wi do
      Compute A and C using Eq. (9)
      prob(t) = cp(t)
      if prob < 0.5 then
        if |A| ⩾ 1 then
          Update Position based on Eq. (11)
        else if |A| < 1
          Update Position based on Eq. (8)
        end if
      else
        Update Position based on Eq. (7)
      end if
      evaluate the population in the objective function using
    Eq. (6) and V_tm, I_tm
    end for
    for all x_wi do//parallel techniques do
      if f_i < f_p then
        x_p = x_wi and f_p = f_i
      end if
    end for
t = t + 1
until t < itern
```

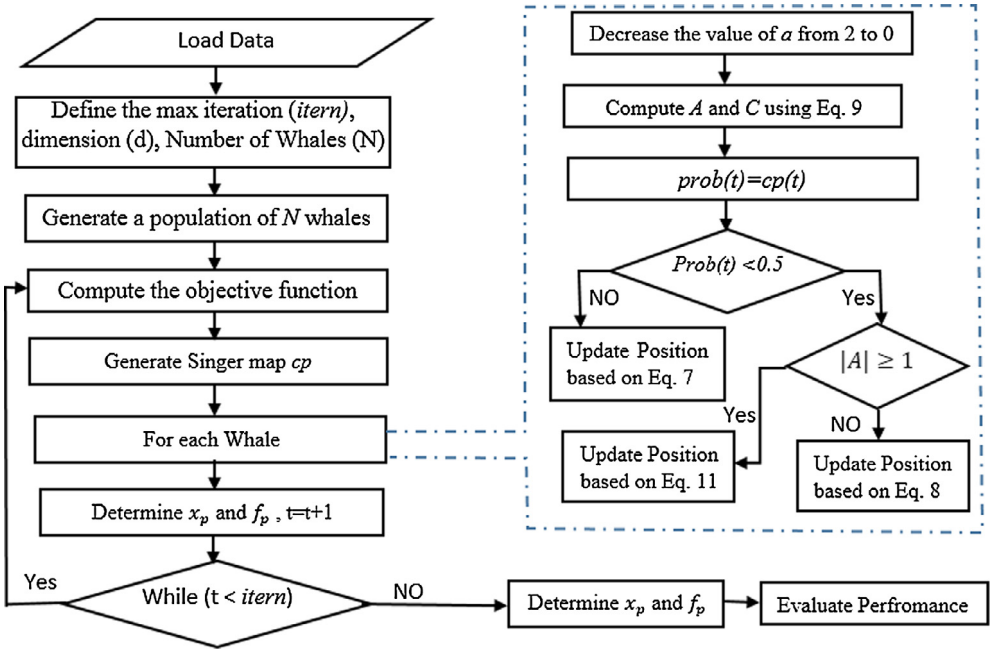

Fig. 3. The Flowchart of CWOA.

6. Experiment and results

To evaluate the performance of the proposed algorithm for identification the parameter of solar cell (SC) models, a standard dataset is used [47]. The results of the CWOA method are compared with some methods mentioned in Section 1, also, to investigate the performance of the proposed method, it is used to extract the parameters of two PV panel datasets taken from [48]. The experiments were implemented in Matlab and run on Windows 7 operative system with 64-bit support with a 2.0 GHz Intel dual-core processor and 4 GB RAM.

6.1. Performance measurement

In order to verify the efficiency and the performance of the proposed approach, it is necessary to define a set of metrics that can be useful for solar cells design. Table 3 enlists seven functions that measure the quality of the estimated parameters. The functions presented are the Relative Error (R_{err}), Normalized Relative Error (NR_{err}), Mean Absolute Error (MAE), Normalized MAE (NMAE), Normalized RMSE (NRMSE), Mean Bias Error (MBE) and Normalized MBE (NMBE). These metrics measures the values of the current obtained from the data of the SC (I_{tm}) and the current estimated (I_{te}) using the parameters obtained by the CWOA. In Table 3, N_E is the number of the experimental data. Meanwhile, min(I_{te}) and max(I_{te}) are minimum and maximum values of I_{te} over N_E.

6.2. Results of CWOA to estimate solar cells parameters

In this experimental section, a dataset that has been extensively studied for this problem is used [54]. In this sense, a commercial silicon solar cell (from the R.T.C. Company of France) with a diameter of 57 mm under the standard test conditions (STC) is used. The following conditions are used in the collection of data: 1 sun (1000 W/m^2) at T = 33 °C. The dataset contains 26 samples and the search domain for unknown parameters of SC models is given in Table 1 and Eq. (13). In this experimental, the parameters of CWOA algorithm are set as N = 150, and the algorithm stops if the global best fitness value remains unchanged in 10% of *itern* (in general *itern* = 10,000 until otherwise stated).

Table 3
Quality indexes used to evaluate the performance of CWOA.

Metric	Formula	Metric	Formula
Relative error (R_{err})	$\frac{I_{tm}-I_{te}}{I_{te}} \times 100$	Normalized RMSE	$\frac{RMSE}{\max(I_{te})-\min(I_{te})}$
Normalized R_{err} (NR_{err})	$\frac{R_{error}}{\max(I_{te})-\min(I_{te})}$	Mean Bias Error (MBE)	$\sum_{i=1}^{N_E} \frac{I_{tm}-I_{te}}{N_E}$
Mean Absolute Error (MAE)	$\sum_{i=1}^{N_E} \frac{\lvert I_{tm}-I_{te}\rvert}{N_E}$	Normalize MBE (NMBE)	$\frac{MBE}{\max(I_{te})-\min(I_{te})}$
Normalized MAE (NMAE)	$\sum_{i=1}^{N_E} \frac{\lvert I_{tm}-I_{te}\rvert/I_{tm}}{N_E}$		

Based on this dataset we study the influence of chaotic maps on the performance of CWOA. Then we compare the results of the CWOA with other two algorithms to estimate the parameters of SD and DD models based on the standard dataset. Also, the results are compared with other results from previous papers. Moreover, four additional temperatures have been included T = 25 °C, T = 50 °C, T = 75 °C and T = 100 °C to verify the efficiency of the proposed approach.

6.2.1. Effect of chaotic map on WOA parameters

The aim of this subsection is to investigate the influence of different control parameters on the CWOA performance. This test is performed using the data for a solar cell. These control parameters including the suitable Chaotic map, A, C and *prob* (with/without chaotic map).

In order to determine the suitable chaotic map, the four chaotic maps namely, Singer, Sinusoidal, Logistic and Tent, are tested. Also, the chaotic map constructs a *cp* (a parameter which assigns to *prob*) with size equal to *itern* (in this experiment is set to 300 iterations). The comparison results between the chaotic maps are given in Table 4, which shows the RMSE and the standard deviation (STD) of the RMSE values obtained using WOA and each chaotic map. From this table, it is observed that Singer map has the lower RMSE and also the STD demonstrates that the results doesn't change along the iterative process, which indicated its stability.

In general, as mentioned above, there are two other parameters *A* and *C* that control the performance of the standard WOA. They should be correctly computed to obtain the best value in the optimization process. Therefore, it is necessary to analyze how these parameters affect the behavior of the method. Several experiments are conducted to test the influence of parameter *C* (where *A* is fixed) based on Singer map (and then test *A* with fixed *C*). In these experiments, the effectiveness of the two parameters is tested at values 2, 1.5, 1 (without chaotic Singer map), also using the chaotic Singer map as a value for each parameter (*A* and *C*) and the three involved parameters (*A, C* and *prob*).

The results of the RMSE and the STD of RMSE for both models are listed in Table 5. From this table, it is observed that the performance of WOA algorithm without chaotic Singer map is better, in general, whenever the value of the parameter A is fixed at 0.5. As well as, the best results for the SD occurs at $C = 1.5$ with RMSE = 0.0010 and an STD of RMSE = 2.2089e−05. Meanwhile, the best results for the DD circuit model is obtained at $C = 1$ and $A = 0.5$ where the RMSE is 0.00105, and the STD of RMSE is 1.1065e−04. On the other hand, in the case of using the chaotic Singer map as value for all parameters of WOA algorithm (i.e. *A, C* and *prob*) as in the last column in Table 5, it can be seen that, the results of RMSE are better than using Singer map for each parameter alone in both models SD and DD. Therefore, from Table 5 it is possible to conclude that, using of chaotic Singer map for parameters *A* and C does not improve the performance of the WOA for estimating the parameters of solar cells, also the performance is not improved when chaos is applied over three variables. However, when chaotic Singer map is used only for *prob* parameter, the CWOA is able to find the best values for the solar cell models as shown in Tables 4 and 5.

6.3. Comparison of CWOA with selected approaches

In this section there are selected some similar optimization approaches that have been selected experimentally considering the similarities that they have and the accuracy in this problem. Moreover, their performance has been tested exhaustively to verify their capabilities [48,53]. These evolutionary approaches are the Bird Matting Optimizer (BMO) [52] and the simplified teaching-learning based optimization (STLBO) [36]. In this context, the results of the CWOA are compared in order to verify its performance and stability. The parameters of each algorithm are set as in the original references except the number of iterations (10,000) and the size of population (150). As well as, each algorithm has been executed 35 times. The results of using the CWOA to identify the parameters of SC using SD and DD models are given in Tables 6–9.

Table 6 shows the quality of the current estimated by the solar cells designed using CWOA, BMO and STBLO methods for both models, as well as, the value of the RMSE and the STD of the RMSE. The results in Table 6 indicate that the CWOA method is consistent and has a high performance to identify the parameters of SD and DD models. In addition, the STBLO gives better RMSE than the CWOA and BMO. However, the STD of RMSE for the CWOA is better than the other algorithms.

In addition, the evolution of the objective function of the three algorithms along the iterative process for the single and double diode model is plotted in Fig. 4. From this figure, it can be seen that, the objective function converges in few iterations, however, to achieve the most accurate value, there are 10,000 iterations. In both cases, SD and DD models (for CWOA), the fitness value becomes relatively not changed and is close to the optimal value after about 5000 iterations. However, at this point, the chaotic map improves the solution accuracy and helps the algorithm to avoid local minima. Moreover, it can be seen the fast convergence of the CWOA for both models, also the convergence of the BMO is better than the convergence of the STBLO method. Based on the measures in Table 6 and Fig. 4, it can be observed the stability of CWOA.

Fig. 5 shows, the current vs. voltage and the power vs. voltage graphs at temperatures 33 °C for the DD and SD models using

Table 4
Evaluation of CWOA using different chaotic maps over the double diode model and the single diode model.

SC model	Index	Chaotic map			
		Singer	Sinusoidal	Logistic	Tent
DD	Mean RMSE	0.1121	0.1145	0.1144	0.1141
	STD RMSE	9.8855e−04	9.88567e−04	6.0739e−04	7.7942e−04
SD	Mean RMSE	0.6562	0.6886	0.7073	0.7511
	STD RMSE	0.0418	0.0589	0.0544	0.0027

Table 5
Results for the effect of parameters A, C and Singer map on the performance of CWOA algorithm.

SC model	Index	A ($C = 0.5$)				C ($A = 0.5$)				ALL
		Singer	2	1.5	1	Singer	2	1.5	1	
SD	Mean RMSE	0.0426	0.0029	0.0030	0.0017	0.0438	0.00174	0.00100	0.00101	0.0014
	STD RMSE	0.0287	0.0015	0.0031	0.0011	0.0389	9.1319e−04	2.2089e−05	4.4756e−05	5.2710e−04
DD	Mean RMSE	0.00147	0.0014	0.0016	0.0014	0.00141	0.001434	0.00133	0.00105	0.0013
	STD RMSE	1.8479e−04	6.7952e−04	3.5580e−04	1.7580e−04	1.2436e−04	1.3329e−04	1.1065e−04	1.1065e−04	2.4034e−04

Table 6
Comparison results between CWOA, BMO and STBLO for DD and SD models.

Model	Algorithm	RMSE	STD RMSE	NRMSE	MAE	NMAE	MBE	NMBE
SD	CWOA	9.8604E-4	1.0216E-8	0.62632	8.28E-4	−0.00533	7.28E−08	11.76653
	BMO	9.8608e−4	3.986 E−05	0.6252	8.48e−04	−0.00635	−1.1302e−06	12.9473
	STBLO	9.8602E−4	1.1333E−7	0.62669	8.29e−04	−0.00537	4.0948e−7	11.79281
DD	CWOA	9.8279E−4	1.1333E−7	0.62972	8.19E−4	−0.00481	1.23263E−7	11.93428
	BMO	9.8262e−4	3.285 E−05	0.6298	8.29 E−04	−0.00480	5.8807 E−07	11.972
	STBLO	9.8248E−4	1.8472E−5	0.62408	8.98e−04	−0.00497	1.3684e−07	11.97524

Table 7
Terminal ($V_t - I_{te}$) measurements and relative error values for SD and DD models.

Data	V_{tm} (V) Measured	I_{tm} (A) Measured	Single Diode (SD) model CWOA			Double Diode (DD) model CWOA		
			I_{te} (A)	R_{err}	NR_{err} % Normalized	I_{te} (A)	R_{err}	NR_{err} % Normalized
1	−0.2057	0.7640	0.7641	−0.0001	37.2740	0.7640	0.0000	39.1382
2	−0.1291	0.7620	0.7627	−0.0007	23.2850	0.7626	−0.0006	24.8540
3	−0.0588	0.7605	0.7614	−0.0009	18.5815	0.7613	−0.0008	19.8312
4	0.0057	0.7605	0.7602	0.0003	47.6379	0.7601	0.0004	48.3955
5	0.0646	0.7600	0.7591	0.0009	62.1028	0.7591	0.0009	62.4836
6	0.1185	0.7590	0.7580	0.0010	62.3786	0.7581	0.0009	62.4934
7	0.1678	0.7570	0.7571	−0.0001	36.9291	0.7571	−0.0001	36.9579
8	0.2132	0.7570	0.7561	0.0009	59.9209	0.7562	0.0008	59.6033
9	0.2545	0.7555	0.7551	0.0004	49.1090	0.7551	0.0004	48.6870
10	0.2924	0.7540	0.7537	0.0003	47.2338	0.7537	0.0003	46.7091
11	0.3269	0.7505	0.7514	−0.0009	17.5153	0.7514	−0.0009	17.1339
12	0.3585	0.7465	0.7474	−0.0009	18.4407	0.7474	−0.0009	18.1278
13	0.3873	0.7385	0.7401	−0.0016	0.0000	0.7401	−0.0016	0.0000
14	0.4137	0.7280	0.7274	0.0006	54.2113	0.7274	0.0006	54.2196
15	0.4373	0.7065	0.7070	−0.0005	27.8785	0.7070	−0.0005	28.4502
16	0.4590	0.6755	0.6753	0.0002	44.7223	0.6753	0.0002	45.5952
17	0.4784	0.6320	0.6307	0.0013	69.5066	0.6307	0.0013	70.5058
18	0.4960	0.5730	0.5719	0.0011	65.3652	0.5719	0.0011	66.4584
19	0.5119	0.4990	0.4996	−0.0006	24.6317	0.4996	−0.0006	25.8178
20	0.5265	0.4130	0.4136	−0.0006	23.5105	0.4136	−0.0006	24.3611
21	0.5398	0.3165	0.3175	−0.0010	14.6464	0.3175	−0.0010	15.1375
22	0.5521	0.2120	0.2122	−0.0002	35.2765	0.2122	−0.0002	35.2708
23	0.5633	0.1035	0.1023	0.0012	69.2550	0.1023	0.0012	68.8513
24	0.5736	−0.0100	−0.0087	−0.0013	8.0300	−0.0087	−0.0013	8.1604
25	0.5833	−0.1230	−0.1255	0.0025	100	−0.1255	0.0025	100
26	0.5900	−0.2100	−0.2085	−0.0015	2.4942	−0.2085	−0.0015	3.7971

Table 8
Comparison results for the SD model.

Parameter	CWOA	BMO	STBLO	HH	GGHS	IGHS	DE	LMSA
I_{ph} (A)	0.76077	0.76077	0.76078	0.7607	0.7609	0.7608	0.7608	0.7608
I_{sd} (μA)	0.3239	0.32479	0.32302	0.3050	0.3262	0.3435	0.3230	0.3185
n	1.4812	1.48173	1.48114	1.4754	1.4822	1.4874	1.4806	1.4798
R_5 (Ω)	0.03636	0.03636	0.03638	0.0366	0.0363	0.0361	0.0364	0.0364
R_{sh} (Ω)	53.7987	53.8716	53.7187	53.5946	53.0647	53.2845	53.7185	53.3264
RMSE	9.8602E−4	9.8608E−4	9.8602E−4	9.9510E−4	9.9097E−4	9.9306E−4	2.3420E−3	9.8640E−4

Table 9
Comparison results for the SD model.

Parameter	SA	CPSO	Rcr-IJADE	GOTLBO	CSO	BFA	ABSO	PS	Newton	ABC
I_{ph} (A)	0.7620	0.7607	0.76086	0.76078	0.7608	0.7602	0.7608	0.7617	0.7608	0.7608
I_{sd} (μA)	0.4798	0.4000	0.32302	0.33155	0.3230	0.8000	0.3062	0.9980	0.3223	0.3251
n	1.5172	1.5033	1.48118	1.48382	1.4812	1.6951	1.4758	1.6000	1.4837	1.4817
R_5 (Ω)	0.0345	0.0354	0.03638	0.03627	0.0364	0.0325	0.0366	0.0313	0.0364	0.0364
R_{sh} (Ω)	43.1034	59.012	53.71853	54.11543	53.7185	50.8691	52.2903	64.1026	53.7634	53.6433
RMSE	0.0190	0.00139	9.8602E−4	9.87442E−4	9.8602E−4	0.029	9.9124E−4	0.0149	9.6960E−3	9.862E−4

the three algorithms. These curves are computed using the parameters estimated by each algorithm. The results from Fig. 5, demonstrate that when the solutions yielded by CWOA are adopted, both solar cell models can accurately represent the characteristics of the real photovoltaic cell than the other two methods. It also indicates that CWOA obtained an accurate approximation for I_{te}.

Table 7 shows the original data, presents the values of the current estimated I_{te} using the parameters obtained by CWOA using the SD and the DD voltage (V_{tm}) and current (I_{tm}) extracted from the real solar cells, at the second and third column, also this table model. The values of both present I_{tm} and I_{te} are compared using the R_{err} and NR_{err}.

In order to investigate the influence of the variation the temperatures on the performance of the proposed method, we test the CWOA at different four temperatures (25, 50, 75 and 100 °C) in addition to 33 °C. However, the temperatures affect the current values in the CWOA and also in the power values, but even with this disturbance, the proposed approach is able to find the best solution as in Fig. 6. From this figure, it is important to mention that, the plots are obtained using the experimental voltage and the computed current presented Table 7. Also, the experimental data has been extensively employed in the related literature [18,54], and the values were extracted under controlled laboratory conditions. It contains negative voltage measurements, for that reason, there are obtained negative power values. The same situation occurs for the plot of current vs. voltage. However, the aim of parameter estimation is reduces the RMSE that is exist between the values contained in the data set and the values computed by

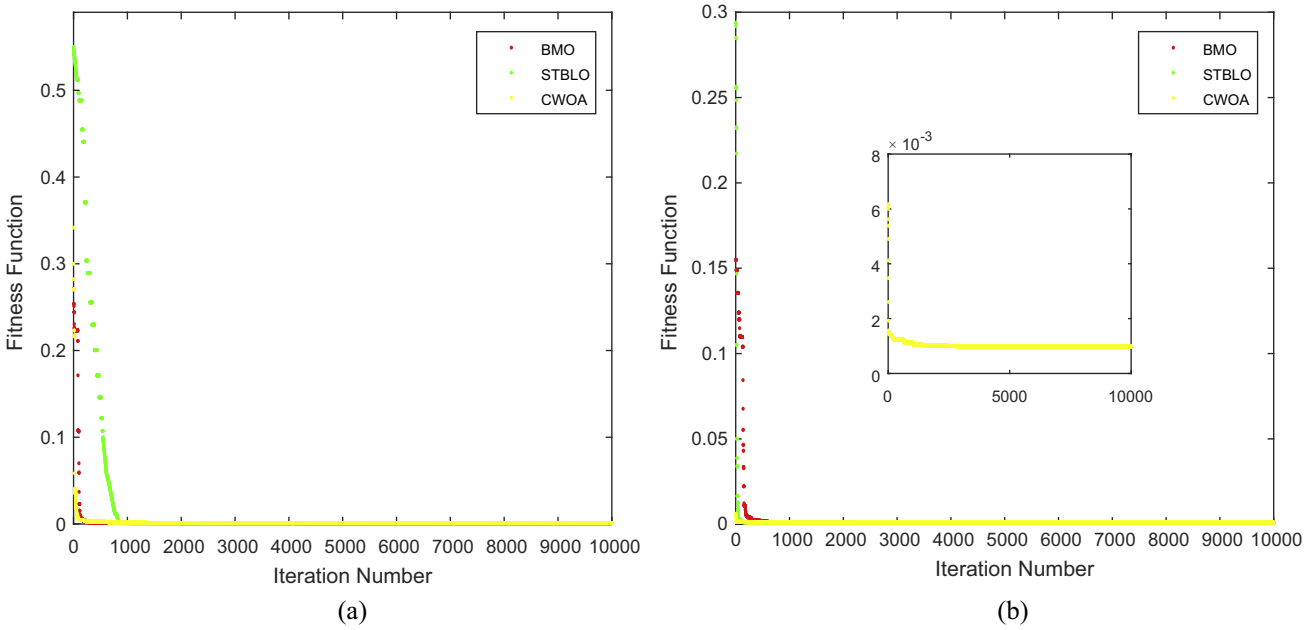

Fig. 4. *RMSE* evolution of CWOA for (a) Single diode model and (b) Double diode model.

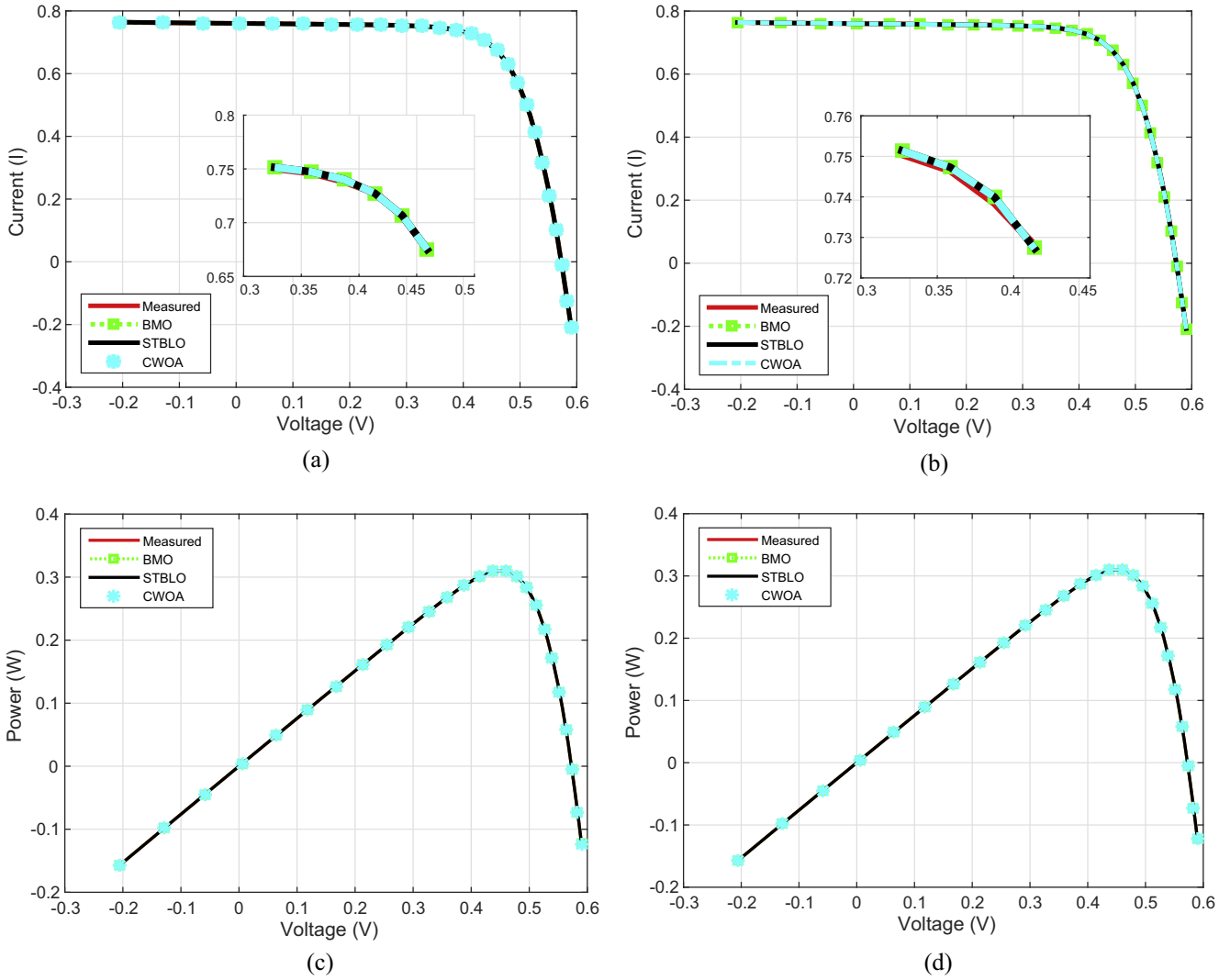

Fig. 5. Measured voltage vs. current computed by using three algorithms For (a) the SD model, (b) the DD model, measured voltage vs. power of three algorithms for (c) the SD model and (d) the DD model.

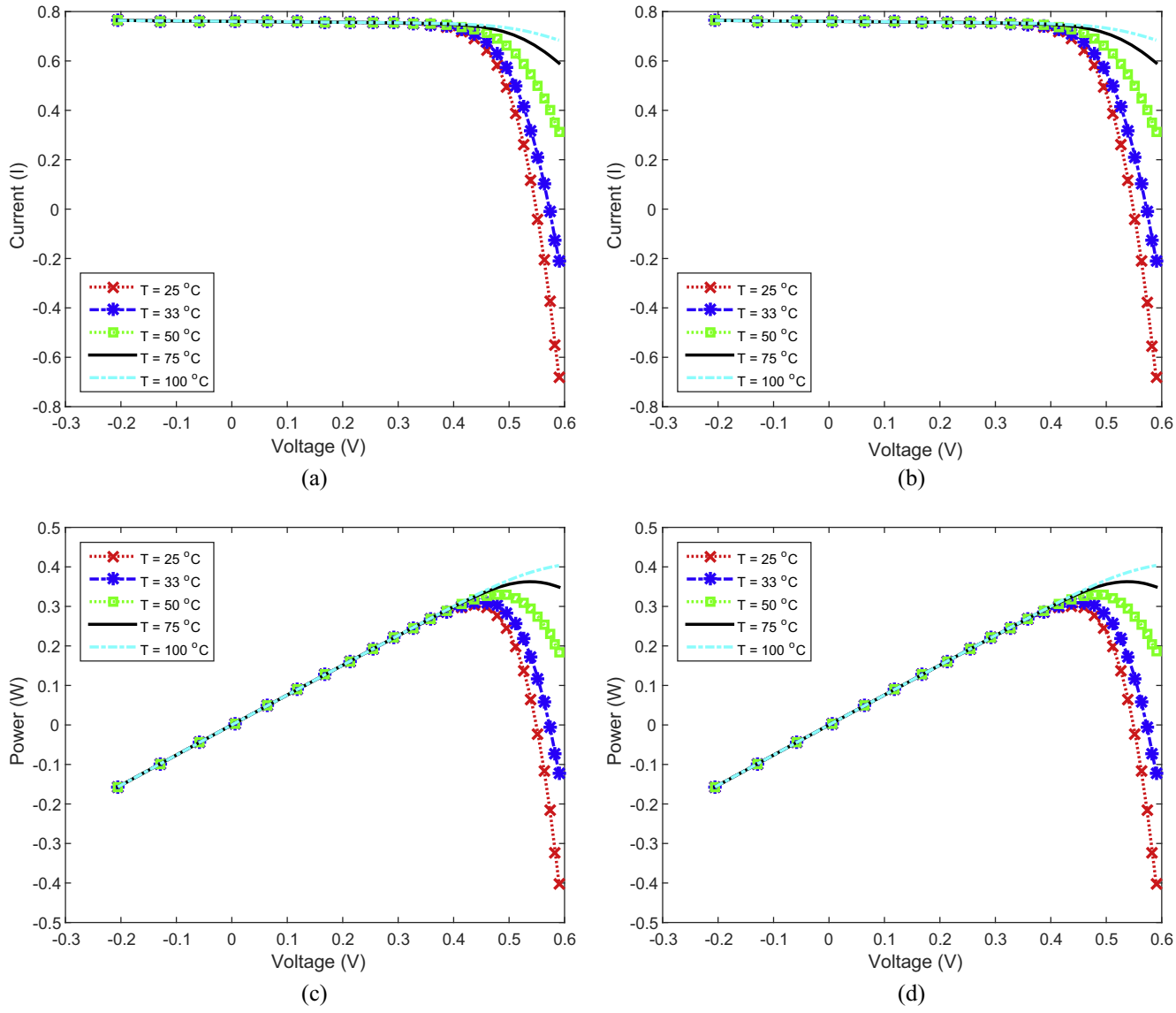

Fig. 6. For the SD model: (a) measured voltage vs. CWOA computed current for different temperatures, (c) measured voltage vs. CWOA-power at various temperatures. For the DD model: (b) measured voltage vs. CWOA computed current for various temperatures, (d) measured voltage vs. CWOA-power at different temperatures.

Table 10
Comparison results for the DD model.

Parameters	CWOA	BMO	STBLO	PS	HS	GGHS	IGHS	ABSO	SA	CSO
I_{ph} (A)	0.76077	0.76078	0.760780	0.7602	0.76176	0.76056	0.76079	0.76078	0.7623	0.76078
I_{sd1} (μA)	0.24150	0.21110	0.225660	0.9889	0.12545	0.37014	0.9731	0.26713	0.4767	0.22732
I_{sd2} (μA)	0.60000	0.87688	0.036740	0.0001	0.2547	0.13504	0.16791	0.38191	0.01	0.72785
n_1	1.45651	1.44533	1.450850	1.6	1.49439	1.49638	1.92126	1.46512	1.5172	1.45151
n_2	1.9899	1.99997	2	1.192	1.49989	1.92998	1.42814	1.98152	2	1.99769
R_S (Ω)	0.03666	0.03682	0.752170	0.032	0.03545	0.03562	0.0369	0.03657	0.0345	0.036737
R_{sh} (Ω)	55.2016	55.8081	55.492000	81.3008	46.82696	62.7899	56.8368	54.6219	43.1034	55.3813
RMSE	9. 8272E−4	9.8262E−4	9.8248E−4	0.01518	0.00126	0.00107	9.8635E−4	9.8344E−4	0.01664	9.8252E−04

the models. CWOA is able to fit the experimental values in all cases no matter how they are obtained.

6.4. Comparisons with related work

The results of the CWOA are compared with other similar methods widely used in the relevant literature as in Tables 8–11 all the results in these tables are taken directly from their corresponding references. The aim of this study is to verify that CWOA is a competitive alternative and is able to find results similar to the related literature. The used approaches are the following: Newton-based method [18], HS [13], GGHS [13], IGHS [13], DE [32], LMSA [49], ABSO [50], PS [51], SA [29], ABC [54], CPSO [35], Rcr-IJADE [32], GOTLBO [53], CSO [37] and BFA [30].

In this sense, Tables 8 and 9 present the comparative study for the SD circuit Based on the RMSE. From these tables, it can be observedthat the RMSE value of CWOA algorithm (9.8602e−4) is smaller than the RMSE of all algorithms except the Rcr-IJADE,

Table 11
Comparison results for the DD model.

Parameters	Rcr-IJADE	GOTLBO	BFA	ABC
I_{ph} (A)	0.760781	0.760752	0.7609	0.7608
I_{sd1} (μA)	0.225974	0.800195	0.0094	0.0407
I_{sd2} (μA)	0.03674	0.036783	0.0453	0.2874
n_1	1.451017	1.448974	1.3809	1.4495
n_2	2	1.999973	1.5255	1.4885
R_S (Ω)	0.749347	0.220462	0.0351	0.0364
R_{sh} (Ω)	55.485443	56.075304	60.0000	53.7804
RMSE	9.8248E−04	9.83177E−4	0.0012	9.861−04

Table 12
The calculated current and its absolute error results using data from solar panel based on monocrystalline.

	Measured		Ref. [48]		BMO		STBLO		CWOA	
	V (V)	I (A)	I (A)	|Error|	I (A)	|Error|	I (A)	|Error|	I (A)	|Error|
1	0.118	1.663	1.6627	0.0003	1.66355	0.00055	1.663809	0.000809	1.663707	0.00070699
2	2.237	1.661	1.659	0.0020	1.659658	0.001342	1.659863	0.001137	1.659879	0.00112094
3	5.434	1.653	1.6531	0.0001	1.65374	0.00074	1.653864	0.000864	1.654054	0.00105408
4	7.26	1.65	1.6497	0.0003	1.650242	0.000242	1.650319	0.000319	1.650601	0.00060093
5	9.68	1.645	1.6445	0.0005	1.644958	4.24E−05	1.644966	3.35E−05	1.645342	0.00034186
6	11.59	1.64	1.6383	0.0017	1.638752	0.001248	1.638696	0.001304	1.63908	0.00092042
7	12.6	1.636	1.633	0.0030	1.633308	0.002692	1.633208	0.002792	1.633549	0.00245133
8	13.37	1.629	1.6267	0.0023	1.626999	0.002001	1.626859	0.002141	1.627132	0.00186827
9	14.09	1.619	1.6171	0.0019	1.618191	0.000809	1.618008	0.000992	1.618186	0.00081413
10	14.88	1.597	1.603	0.0060	1.603215	0.006215	1.602976	0.005976	1.603013	0.00601267
11	15.59	1.581	1.582	0.0010	1.581971	0.000971	1.581677	0.000677	1.581569	0.00056926
12	16.4	1.542	1.5432	0.0012	1.542992	0.000992	1.542643	0.000643	1.542382	0.00038249
13	16.71	1.524	1.5225	0.0015	1.521923	0.002077	1.52156	0.00244	1.521265	0.00273541
14	16.98	1.5	1.5006	0.0006	1.499962	3.8E−05	1.499596	0.000404	1.499281	0.00071863
15	17.13	1.485	1.4867	0.0017	1.486047	0.001047	1.485685	0.000685	1.485367	0.00036715
16	17.32	1.465	1.4674	0.0024	1.466409	0.001409	1.466056	0.001056	1.465748	0.00074819
17	17.91	1.388	1.3897	0.0017	1.388083	8.27E−05	1.387824	0.000176	1.387651	0.00034921
18	19.08	1.118	1.1208	0.0028	1.116958	0.001042	1.117581	0.000419	1.118199	0.00019866

Table 13
The estimated parameters and their accuracy for the dataset from solar panel based on monocrystalline.

Parameter	Ref. [48]	BMO	STBLO	CWOA
R_S (m)	4.879	5.00	5.00	5.00
R_p	15.419	14.9371	15.40	15.4
I_p	1.4142	1.6646	1.7000	1.7
I_{sd} (μ)	1.6635	1.4311	1.4127	1.6338
n	1.4986	1.4994	1.5	1.5
MAE	0.001722	0.001308	0.00127	0.00122003
RMSE	0.002181	0.001900	0.001900	0.0018
NMAE	0.00153	0.000838	0.000804	0.00076963
NRMSE	0.004026	0.003476	0.003478	0.00329967
MBE	0.000222	−5.32E−05	4.50E−05	−2.18E−07

CSO and STLBO algorithms which have the same RMSE value. However, the BMO in the second rank and it is better than the RMSE values of the rest algorithms. Also, PS and BFA algorithms are the worst results which have RMSE equal to 0.0149 and 0.029 respectively.

On the other hand, the same methods have been applied to the DD model as in Tables 9 and 10 which show that the CWOA algorithm yields the best performance compared to other algorithms based on the value of RMSE. The value of CWOA is close to the values of Rcr-IJADE, CSO, BMO and STLBO, but it is obviously less than other methods.

Moreover, when the Tables 8–11 are compared, it is possible to observe that the performance of CWOA for DD model is better than for SD model. Therefore, these results indicate that CWOA algorithm has the ability to accurately find an optimal result for the parameter identification problem of solar cell models. It is important to mention that not all the algorithms selected for comparisons have been used in the related literature for DD models, for that reason, they are not employed in Tables 10 and 11.

6.5. CWOA on PV panels

In order to establish the ability of the proposed method to work in other real applications, in this experimental section, we extended the CWOA to extract the parameters of two PV panels (a Polycrystalline and Monocrystalline) [48] (the definition of PV panels is given in Appendix A). The *I-V* data is measured from each panel based on values of the voltage (V_{oc}) and the current (I_{SC}) when the cells are open-circuited and short-circuited, respectively. The results of CWOA are compared with BMO, STBLO and the results presented in Ref. [48].

6.5.1. Parameter estimation of monocrystalline PV panels

In this experiment a commercial solar panel model STM6-40/36 manufactured by Schutten Solar is selected to assess the performance of CWOA in practice [48]. The panel used in this experiment consists of 36 Monocrystalline cells (of size 38 mm × 128 mm) aligned in series. The dataset is measured from this solar panel model at Temperature 51 °C, as given in Table 12 (in the second

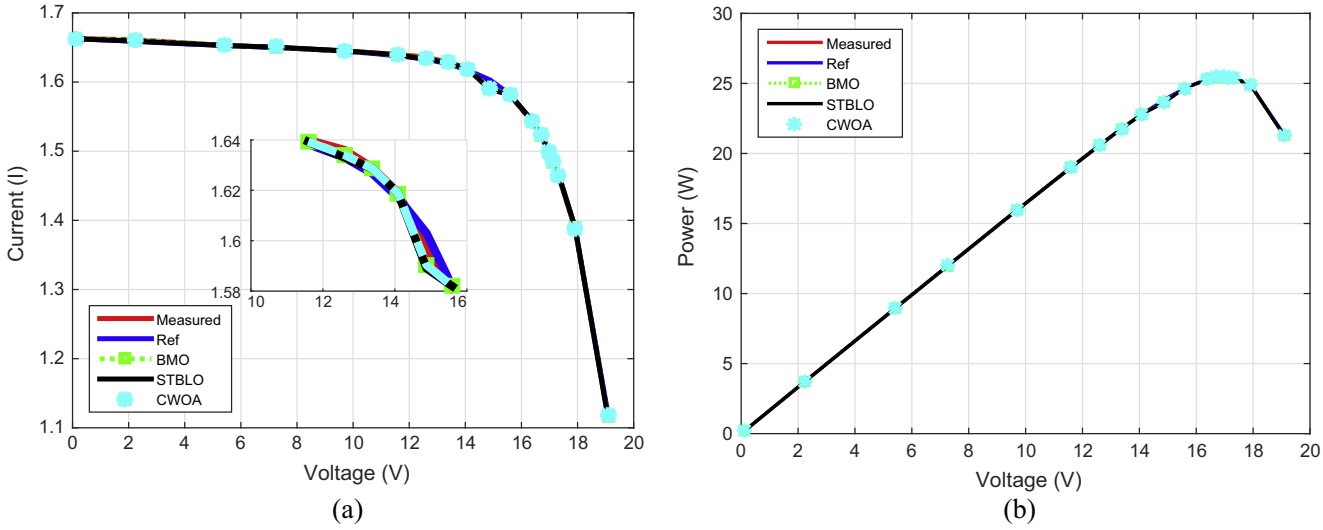

Fig. 7. The computed (a) current and (b) power by each algorithm using solar panel based on monocrystalline.

Table 14
The calculated current and its absolute error results using data from solar panel based on polycrystalline.

	Measured		Ref. [48]		BMO		STBLO		CWOA	
	V (V)	I (A)	I (A)	|Error|	I (A)	|Error|	I(A)	|Error|	I (A)	|Error|
1	17.65	3.83	3.836	0.006	3.836857	0.006857	3.859808	0.029808	3.829267	0.000733
2	17.41	4.29	4.28	0.01	4.266148	0.023852	4.275046	0.014954	4.271842	0.018158
3	17.25	4.56	4.5541	0.0059	4.538999	0.021001	4.542195	0.017805	4.549452	0.010548
4	17.1	4.79	4.794	0.004	4.782374	0.007626	4.7822	0.0078	4.789196	0.000804
5	16.9	5.07	5.093	0.023	5.084525	0.014525	5.081869	0.011869	5.090341	0.020341
6	16.76	5.27	5.287	0.017	5.274076	0.004076	5.269857	0.000143	5.282832	0.012832
7	16.34	5.75	5.794	0.044	5.785045	0.035045	5.781437	0.031437	5.785727	0.035727
8	16.08	6	6.055	0.055	6.048503	0.048503	6.046476	0.046476	6.058983	0.058983
9	15.71	6.36	6.3691	0.0091	6.352108	0.007892	6.351531	0.008469	6.360167	0.000167
10	15.39	6.58	6.5881	0.0081	6.572322	0.007678	6.574001	0.005999	6.580138	0.000138
11	14.93	6.83	6.8334	0.0034	6.819291	0.010709	6.823392	0.006608	6.852843	0.022843
12	14.58	6.97	6.9748	0.0048	6.962603	0.007397	6.967842	0.002158	6.966552	0.003448
13	14.17	7.1	7.1014	0.0014	7.090987	0.009013	7.096757	0.003243	7.091704	0.008296
14	13.59	7.23	7.2265	0.0035	7.218298	0.011702	7.223823	0.006177	7.247228	0.017228
15	13.16	7.29	7.2898	0.0002	7.283106	0.006894	7.288017	0.001983	7.2908	0.0008
16	12.74	7.34	7.3345	0.0055	7.328875	0.011125	7.333003	0.006997	7.344432	0.004432
17	12.36	7.37	7.3643	0.0057	7.359526	0.010474	7.362914	0.007086	7.364256	0.005744
18	11.81	7.38	7.3947	0.0147	7.391063	0.011063	7.393434	0.013434	7.380486	0.000486
19	11.17	7.41	7.4174	0.0074	7.414487	0.004487	7.415816	0.005816	7.409522	0.000478
20	10.32	7.44	7.4352	0.0048	7.432922	0.007078	7.433183	0.006817	7.435266	0.004734
21	9.74	7.42	7.4426	0.0226	7.440792	0.020792	7.440508	0.020508	7.427906	0.007906
22	9.06	7.45	7.4487	0.0013	7.447095	0.002905	7.446314	0.003686	7.448784	0.001216

and third columns), where the $I_{SC} = 1.663$ A, $V_{OC} = 21.02$ V, terminal voltage ($V_M = 16.98$ V) and the output current ($I_M = 1.50$ A) of the panels operating at the maximum power point (MPP).

The comparison results of the CWOA and the other algorithms based on a set of measures are given in Tables 12 and 13, as well as; the current is computed based on the extracted parameters using each algorithm. From these tables it can be seen that the CWOA has better values for RMSE, NRMSE, MAE, NMAE, MBE and the absolute error expressed (|Error|). Also, the STBLO is better than both the BMO and the results from [48] (we used the word *Ref* to point to the results of [48]).

Fig. 7 shows the current vs. voltage and power vs. voltage graphs at temperatures 51 °C for the SD model after estimating the parameters using each algorithm. From this figure, it can be observed that the BMO, CWOA, and STBLOare better than *Ref*. However, all of them don't reach the measured curve from point 6 to point 10, but in general, the CWOA is the closest to the measured values.

Table 15
The estimated parameters and their accuracy for the dataset from solar panel based on polycrystalline.

Parameter	Ref.[48]	BMO	STBLO	CWOA
R_S (m)	4.9	0.0049	0.0055	0.0049
R_p	9.745	9.7000	9.8000	9.7942
I_{sd} (μ)	7.4838	7.4763	7.4814	7.4760
I_p	1.2	1.2333	1.1679	1.2
n	1.2072	1.2092	1.2048	1.2069
MAE	0.0117	0.013213	0.011785	0.010729
RMSE	0.017879	0.016985	0.016211	0.017601
NMAE	0.001058	0.001195	0.001068	0.000969
NRMSE	0.004949	0.004705	0.00452	0.004863
MBE	−0.00835	−9.1 E-08	−0.0027	−0.00581

6.5.2. Parameters estimation of polycrystalline PV panels

This experiment is performed by using a commercial solar panel model STM6-120/36 manufactured by Schutten Solar which consists of 36 polycrystalline cells (of size 156 mm × 156 mm) in

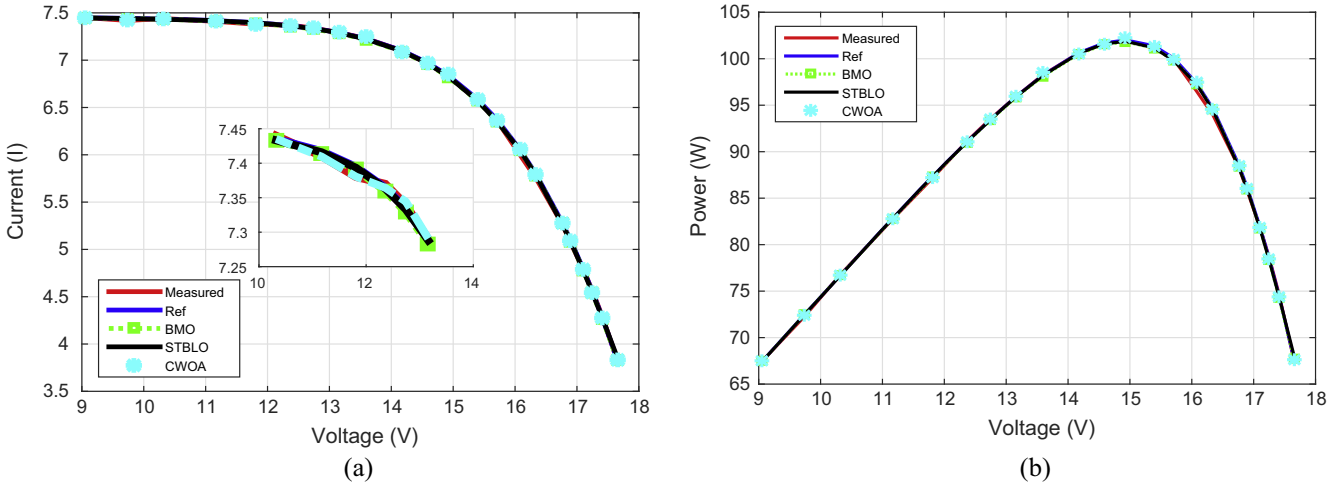

Fig. 8. The computed current and power by each algorithm using solar panel based on polycrystalline.

series form. The dataset measured using this panel contains 22 points which is measured as at Temperature 55 °C, $I_{SC} = 7.48$ A, $V_{OC} = 19.21$ V, $V_M = 14.93$ V and $I_M = 6.83$ A, the data is given in Table 14 (in the second and third columns).

Tables 14 and 15 show the computed current and extracted parameters of the solar panel using the algorithms. From these tables, we can see that the results of *Ref* are better than both the BMO and the STBLO algorithms. However, the best results are the values of CWOA method.

In addition to, the current and the power are plotted against the voltage as shown in Fig. 8, also from this figure it can be seen that the CWOA curve is very close to the measurement curve. However, the rest algorithms are failed to be close to the measured curve as shown in the current curve (Fig. 8(a)) from point 15 to point 19.

7. Conclusions

In this paper, a new approach is introduced to estimate the parameters of solar cells and photovoltaic modules or panels. The proposed approach is called Chaotic Whale Optimization Algorithm (CWOA) which uses the chaotic Singer map to improve the performance of WOA. The CWOA then is used to find the best configuration to the parameters of solar cells and PV modules using the RMSE as the objective function. In order to analyze the performance and stability, the CWOA has been tested using real data extracted from solar cells and PV panels.

The effects of chaotic Singer map in the WOA parameters are studied, in which it can be observed that whenever the chaotic map is used for all parameters of WOA, the results are better than if it is utilized for the parameters A and C (in alone form). However, the accuracy of applying Singer map to the parameter *prob* only is better than if it is applied to all parameters of WOA the CWOA.

Moreover, the experimental results of the proposed approach have been compared with other similar techniques widely used in the literature to estimate the parameters of solar cells. From these results, it can be concluded that the performance of CWOA algorithm is close to the results of Rcr-IJADE, CSO, BMO and STLBO for estimating the parameters of SD and DD models, and even it is better than all other algorithms used for comparison. An additional test has been performed to verify the stability of the CWOA. In this test, the proposed approach is compared only with STBLO and BMO, the experimental results provide an evidence that the values obtained by CWOA are better. This fact occurs based on the using of Singer chaotic map; it helps the WOA to avoid the local optimal and improving its convergences. This behavior is supported by different metrics. Moreover, when CWOA is used to estimate the parameters of PV panels, the results are better than those of other similar app I_M roaches.

In future work, the proposed method will be implemented other interesting models for solar cells. Also, some other modification will be introduced, extending the using of optimization algorithms for renewable energy problems.

Acknowledgements

The second author acknowledges the National High-tech R&D Program of China (863 Program) (Grant No. 2015AA015403) and Nature Science Foundation of Hubei Province (Grant No. 2015CFA059) for partially support this research.

Appendix A

A.1. PV panels

A PV panel consists of M solar cells interconnected in series form. The current of the panel I is equal to. Considering that the M cells are received, the same level of photon flux [48], then the same voltage and current are produced from these cells.

In the related literature, it is common to use the SD model for each element of the PV panel. Considering this fact, to compute the current of the entire PV panel, the *I-V* relation presented in Eq. (3) can be written as:

$$I_{te} = I_{ph} - I_{sd}\left[\exp\left(\frac{(V_t + M \cdot R_s \cdot I_{te})}{n \cdot k \cdot T \cdot M/q}\right) - 1\right] - \frac{V_t + M \cdot R_s \cdot I_{te}}{M \cdot R_{sh}} \quad (A.1)$$

References

[1] Renewables 2016: global status report; 2016. http://www.ren21.net/wp-content/uploads/2016/10/REN21_GSR2016_FullReport_en_11.pdf.

[2] Navabi R, Abedi S, Hosseinian SH, Pal R. On the fast convergence modeling and accurate calculation of PV output energy for operation and planning studies. Energy Convers Manage 2015;89:497–506. http://dx.doi.org/10.1016/j.enconman.2014.09.070.

[3] Ma T, Yang H, Lu L. Solar photovoltaic system modeling and performance prediction. Renew Sustain Energy Rev 2014;36:304–15. http://dx.doi.org/10.1016/j.rser.2014.04.057.

[4] Lo Brano V, Orioli A, Ciulla G, Di Gangi A. An improved five-parameter model for photovoltaic modules. Sol Energy Mater Sol Cells 2010;94:1358–70. http://dx.doi.org/10.1016/j.solmat.2010.04.003.

[5] Han L, Koide N, Chiba Y, Islam A, Mitate T. Modeling of an equivalent circuit for dye-sensitized solar cells: improvement of efficiency of dye-sensitized solar

cells by reducing internal resistance. Comptes Rendus Chim 2006;9:645–51. http://dx.doi.org/10.1016/j.crci.2005.02.046.
[6] Villalva MG, Gazoli JR, Filho ER. Comprehensive approach to modeling and simulation of photovoltaic arrays. IEEE Trans Power Electron 2009;24:1198–208.
[7] Huld T, Gottschalg R, Beyer HG, Topič M. Mapping the performance of PV modules, effects of module type and data averaging. Sol Energy 2010;84:324–38. http://dx.doi.org/10.1016/j.solener.2009.12.002.
[8] Xiao W, Lind MGJ, Dunford WG, Capel A. Real-time identification of optimal operating points in photovoltaic power systems. IEEE Trans Ind Electron 2006;53:1017–26. http://dx.doi.org/10.1109/TIE.2006.878355.
[9] Chegaar M, Ouennoughi Z, Guechi F, Langueur H. Determination of solar cells parameters under illuminated conditions. J Electron Dev 2003;2:17–21.
[10] Ye M, Wang X, Xu Y. Parameter extraction of solar cells using particle swarm optimization. J Appl Phys 2009;105. http://dx.doi.org/10.1063/1.3122082.
[11] Djamila R, Matagne E. Optimization of photovoltaic power systems: modelization. Simulation and control. London: Springer-Verlag; 2012. http://dx.doi.org/10.1007/978-1-4471-2403-0.
[12] Ishaque K, Salam Z, Mekhilef S, Shamsudin A. Parameter extraction of solar photovoltaic modules using penalty-based differential evolution. Appl Energy 2012;99:297–308. http://dx.doi.org/10.1016/j.apenergy.2012.05.017.
[13] Askarzadeh A, Rezazadeh A. Parameter identification for solar cell models using harmony search-based algorithms. Sol Energy 2012;86:3241–9. http://dx.doi.org/10.1016/j.solener.2012.08.018.
[14] Allam D, Yousri DA, Eteiba MB. Parameters extraction of the three diode model for the multi-crystalline solar cell/module using Moth-flame optimization algorithm. Energy Convers Manage 2016;123:535–48. http://dx.doi.org/10.1016/j.enconman.2016.06.052.
[15] Jun-Hua L, Ming L. An analysis on convergence and convergence rate estimate of elitist genetic algorithms in noisy environments. Optik (Stuttg) 2013;124:6780–5. http://dx.doi.org/10.1016/j.ijleo.2013.05.101.
[16] Pan H, Wang L, Liu B. Particle swarm optimization for function optimization in noisy environment. Appl Math Comput 2006;181:908–19. http://dx.doi.org/10.1016/j.amc.2006.01.066.
[17] Niu Q, Zhang L, Li K. A biogeography-based optimization algorithm with mutation strategies for model parameter estimation of solar and fuel cells. Energy Convers Manage 2014;86:1173–85. http://dx.doi.org/10.1016/j.enconman.2014.06.026.
[18] Easwarakhanthan T, Bottin J, Bouhouch I, Boutrit C. Nonlinear minimization algorithm for determining the solar cell parameters with microcomputers. Int J Sol Energy 1986;4:1–12. http://dx.doi.org/10.1080/01425918608909835.
[19] Ortiz-Conde A, García Sánchez FJ, Muci J. New method to extract the model parameters of solar cells from the explicit analytic solutions of their illuminated I-V characteristics. Sol Energy Mater Sol Cells 2006;90:352–61. http://dx.doi.org/10.1016/j.solmat.2005.04.023.
[20] Gao X, Cui Y, Hu J, Xu G, Yu Y. Lambert W-function based exact representation for double diode model of solar cells: comparison on fitness and parameter extraction. Energy Convers Manage 2016;127:443–60. http://dx.doi.org/10.1016/j.enconman.2016.09.005.
[21] Chan DSH, Phillips JR, Phang JCH. A comparative study of extraction methods for solar cell model parameters. Solid State Electron 1986;29:329–37. http://dx.doi.org/10.1016/0038-1101(86)90212-1.
[22] Orioli A, Di Gangi A. A procedure to calculate the five-parameter model of crystalline silicon photovoltaic modules on the basis of the tabular performance data. Appl Energy 2013;102:1160–77. http://dx.doi.org/10.1016/j.apenergy.2012.06.036.
[23] Appelbaum J, Peled A. Parameters extraction of solar cells – a comparative examination of three methods. Sol Energy Mater Sol Cells 2014;122:164–73. http://dx.doi.org/10.1016/j.solmat.2013.11.011.
[24] Li Y, Huang W, Huang H, Hewitt C, Chen Y, Fang G, et al. Evaluation of methods to extract parameters from current-voltage characteristics of solar cells. Sol Energy 2013;90:51–7. http://dx.doi.org/10.1016/j.solener.2012.12.005.
[25] Elbaset AA, Ali H, Abd-El Sattar M. Novel seven-parameter model for photovoltaic modules. Sol Energy Mater Sol Cells 2014;130:442–55. http://dx.doi.org/10.1016/j.solmat.2014.07.016.
[26] Alam DF, Yousri DA, Eteiba MB. Flower pollination algorithm based solar PV parameter estimation. Energy Convers Manage 2015;101:410–22. http://dx.doi.org/10.1016/j.enconman.2015.05.074.
[27] AlRashidi MR, AlHajri MF, El-Naggar KM, Al-Othman AK. A new estimation approach for determining the I-V characteristics of solar cells. Sol Energy 2011;85:1543–50. http://dx.doi.org/10.1016/j.solener.2011.04.013.
[28] Jervase JA, Bourdoucen H, Al-Lawati A. Solar cell parameter extraction using genetic algorithms. Meas Sci Technol 2001;12:1922–5. http://dx.doi.org/10.1088/0957-0233/12/11/322.
[29] El-Naggar KM, AlRashidi MR, AlHajri MF, Al-Othman AK. Simulated annealing algorithm for photovoltaic parameters identification. Sol Energy 2012;86:266–74. http://dx.doi.org/10.1016/j.solener.2011.09.032.
[30] Rajasekar N, Krishna Kumar N, Venugopalan R. Bacterial foraging algorithm based solar PV parameter estimation. Sol Energy 2013;97:255–65. http://dx.doi.org/10.1016/j.solener.2013.08.019.
[31] Jiang LL, Maskell DL, Patra JC. Parameter estimation of solar cells and modules using an improved adaptive differential evolution algorithm. Appl Energy 2013;112:185–93. http://dx.doi.org/10.1016/j.apenergy.2013.06.004.
[32] Gong W, Cai Z. Parameter extraction of solar cell models using repaired adaptive differential evolution. Sol Energy 2013;94:209–20. http://dx.doi.org/10.1016/j.solener.2013.05.007.
[33] Siddiqui MU, Abido M. Parameter estimation for five- and seven-parameter photovoltaic electrical models using evolutionary algorithms. Appl Soft Comput J 2013;13:4608–21. http://dx.doi.org/10.1016/j.asoc.2013.07.005.
[34] Zagrouba M, Sellami A, Bouaïcha M, Ksouri M. Identification of PV solar cells and modules parameters using the genetic algorithms: application to maximum power extraction. Sol Energy 2010;84:860–6. http://dx.doi.org/10.1016/j.solener.2010.02.012.
[35] Wei H, Cong J, Lingyun X. Extracting solar cell model parameters based on chaos particle swarm algorithm. In: Int conf electr inf control eng (ICEICE). p. 398–402. http://dx.doi.org/10.1109/ICEICE.2011.5777246.
[36] Niu Q, Zhang H, Li K. An improved TLBO with elite strategy for parameters identification of PEM fuel cell and solar cell models. Int J Hydrogen Energy 2014;39:3837–54. http://dx.doi.org/10.1016/j.ijhydene.2013.12.110.
[37] Guo L, Meng Z, Sun Y, Wang L. Parameter identification and sensitivity analysis of solar cell models with cat swarm optimization algorithm. Energy Convers Manage 2016;108:520–8. http://dx.doi.org/10.1016/j.enconman.2015.11.041.
[38] Wolpert DH, Macready WG. No free lunch theorems for optimization. IEEE Trans Evol Comput 1997;1:67–82. http://dx.doi.org/10.1109/4235.585893.
[39] Hrstka O, Kučerová A. Improvements of real coded genetic algorithms based on differential operators preventing premature convergence. Adv Eng Softw 2004;35:237–46. http://dx.doi.org/10.1016/S0965-9978(03)00113-3.
[40] Ostadmohammadi Arani B, Mirzabeygi P, Shariat Panahi M. An improved PSO algorithm with a territorial diversity-preserving scheme and enhanced exploration-exploitation balance. Swarm Evol Comput 2013;11:1–15. http://dx.doi.org/10.1016/j.swevo.2012.12.004.
[41] Qing L, Gang W, Zaiyue Y, Qiuping W. Crowding clustering genetic algorithm for multimodal function optimization. Appl Soft Comput J 2008;8:88–95. http://dx.doi.org/10.1016/j.asoc.2006.10.014.
[42] Li M, Lin D, Kou J. A hybrid niching PSO enhanced with recombination-replacement crowding strategy for multimodal function optimization. Appl Soft Comput J 2012;12:975–87. http://dx.doi.org/10.1016/j.asoc.2011.11.032.
[43] Niksirat M, Ghatee M, Mehdi Hashemi S. Multimodal K-shortest viable path problem in Tehran public transportation network and its solution applying ant colony and simulated annealing algorithms. Appl Math Model 2012;36:5709–26. http://dx.doi.org/10.1016/j.apm.2012.01.007.
[44] Wang C-M, Huang Y-F. Self-adaptive harmony search algorithm for optimization. Expert Syst Appl 2010;37:2826–37. http://dx.doi.org/10.1016/j.eswa.2009.09.008.
[45] Beyer H-G. Evolutionary algorithms in noisy environments: theoretical issues and guidelines for practice. Comput Methods Appl Mech Eng 2000;186:239–67. http://dx.doi.org/10.1016/S0045-7825(99)00386-2.
[46] Mirjalili S, Lewis A. The whale optimization algorithm. Adv Eng Softw 2016;95:51–67. http://dx.doi.org/10.1016/j.advengsoft.2016.01.008.
[47] Yang D, Li G, Cheng G. On the efficiency of chaos optimization algorithms for global optimization. Chaos, Solitons Fractals 2007;34:1366–75. http://dx.doi.org/10.1016/j.chaos.2006.04.057.
[48] Tong NT, Pora W. A parameter extraction technique exploiting intrinsic properties of solar cells. Appl Energy 2016;176:104–15. http://dx.doi.org/10.1016/j.apenergy.2016.05.064.
[49] Dkhichi F, Oukarfi B, Fakkar A, Belbounaguia N. Parameter identification of solar cell model using Levenberg-Marquardt algorithm combined with simulated annealing. Sol Energy 2014;110:781–8. http://dx.doi.org/10.1016/j.solener.2014.09.033.
[50] Askarzadeh A, Rezazadeh A. Artificial bee swarm optimization algorithm for parameters identification of solar cell models. Appl Energy 2013;102:943–9. http://dx.doi.org/10.1016/j.apenergy.2012.09.052.
[51] AlHajri MF, El-Naggar KM, AlRashidi MR, Al-Othman AK. Optimal extraction of solar cell parameters using pattern search. Renew Energy 2012;44:238–45. http://dx.doi.org/10.1016/j.renene.2012.01.082.
[52] Askarzadeh A, Rezazadeh A. Extraction of maximum power point in solar cells using bird mating optimizer-based parameters identification approach. Sol Energy 2013;90:123–33. http://dx.doi.org/10.1016/j.solener.2013.01.010.
[53] Chen X, Yu K, Du W, Zhao W, Liu G. Parameters identification of solar cell models using generalized oppositional teaching learning based optimization. Energy 2016;99:170–80. http://dx.doi.org/10.1016/j.energy.2016.01.052.
[54] Oliva D, Cuevas E, Pajares G. Parameter identification of solar cells using artificial bee colony optimization. Energy 2014;72:93–102. http://dx.doi.org/10.1016/j.energy.2014.05.011.
[55] Jordehi AR. Parameter estimation of solar photovoltaic (PV) cells: a review. Renew Sustain Energy Rev 2016;61:354–71. http://dx.doi.org/10.1016/j.rser.2016.03.049.
[56] Jain A, Kapoor A. Exact analytical solutions of the parameters of real solar cells using Lambert W-function. Sol Energy Mater Sol Cells 2004;81:269–77. http://dx.doi.org/10.1016/j.solmat.2003.11.018.
[57] Saleem H, Karmalkar S. An analytical method to extract the physical parameters of a solar cell from four points on the illuminated J-V curve. IEEE Electron Device Lett 2009;30:349–52. http://dx.doi.org/10.1109/LED.2009.2013882.
[58] Saremi S, Mirjalili S, Lewis A. Biogeography-based optimisation with chaos. Neural Comput Appl 2014;25:1077–97. http://dx.doi.org/10.1007/s00521-014-1597-x.